Functional Roles of Conserved Residues in the Unstructured Loop of *Vibrio harveyi* Bacterial Luciferase†

John C. Low and Shiao-Chun Tu*

Department of Biology and Biochemistry, University of Houston, Houston, Texas 77204-5001

Received October 22, 2001

ABSTRACT: Residues 257−291 of the *Vibrio harveyi* bacterial luciferase α subunit comprise a highly conserved, protease-labile, disordered loop region, most of which is unresolved in the previously determined X-ray structures of the native enzyme. This loop region has been shown to display a time- dependent proteolysis resistance upon single catalytic turnover and was postulated to undergo conformational changes during catalysis ([AbouKhair, N. K., Ziegler, M. M., and Baldwin, T. O. (1985) *Biochemistry 24*, 3942−3947]. To investigate the role of this region in catalysis, we have performed site-specific mutations of different conserved loop residues. In comparison with V_{max} and $V_{max}/K_{m,flavin}$ of the native luciferase, the bioluminescence activities of αG284P were decreased to 1−2% whereas those of αG275P and αF261D were reduced by 4−6 orders of magnitude. Stopped-flow results indicate that both αG275P and αF261D were able to form the 4a-hydroperoxy-FMN intermediate II but at lower yields. Both mutants also had enhanced rates for the intermediate II nonproductive dark decay and significantly compromised abilities to oxidize the decanal substrate. Additional mutations were introduced into the αG275 and αF261 positions, and the activities of the resulting mutants were characterized. Results indicate that the torsional flexibility of the αG275 residue and the bulky and hydrophobic nature of the αF261 residue were critical to the luciferase activity. Our results also support a functional role for the α subunit unstructured loop itself, possibly by serving as a mobile gating mechanism in shielding critical intermediates (including the excited flavin emitter) from exposure to medium.

Bacterial luciferase is a flavin-dependent monooxygenase that catalyzes the reaction of reduced riboflavin 5′-phosphate ($FMNH_2$),[1] O_2, and a long-chain aliphatic aldehyde to produce FMN, H_2O, and the corresponding aliphatic acid with a concomitant emission of blue-green light ($\lambda_{max} = 490$ nm). A proposed mechanism (Scheme 1) for the light-emitting reaction has been the subject of considerable investigation (*1* and references cited therein). Of critical importance to the luminescence reaction is the generation of the 4a-hydroperoxy-FMN intermediate II species and its subsequent reaction with an aliphatic aldehyde, ultimately leading to the formation of the excited 4a-hydroxy-FMN emitter (intermediate IV*).

The native luciferase from *Vibrio harveyi* is a 77 kDa heterodimer with the α and *β* subunits having molecular masses of 40 and 37 kDa, respectively (*2*). The adjacent *luxA* and *luxB* genes in the *lux* operon encode the corresponding α and *β* subunits and are likely a result of gene duplication (*3*). The α and *β* polypeptides display 32% sequence identity, and the α carbon chains of the two subunits are nearly superimposable. However, the *V. harveyi* luciferase *αβ* dimer has a single active site that binds one molecule of reduced flavin (*4*, *5*) and an aldehyde (*6*) as substrates. In addition, this luciferase also binds an aldehyde inhibitor that competes against the $FMNH_2$ substrate (*6*). A number of "essential" amino acid residues in luciferase have been identified by chemical modifications and mutageneses, with almost all of them located in the luciferase α subunit (*7* and references cited therein). Hence, the single active site is considered to reside primarily, or exclusively, in the α subunit. Such a conjecture has also been reached by comparing the luciferase X-ray structure with other similar protein motifs (*8*, *9*).

The main distinguishing feature of the 355-residue α subunit and the 324-residue *β* subunit is a 29-residue insert in the α subunit between two residues corresponding to the residues 258 and 259 on the *β* subunit (*10*, *11*). Consistent with a high mobility, most of this region is not resolved in the previously determined X-ray structures of the native enzyme (*8*, *9*). In the absence of substrate, this region is subject to proteolytic cleavage between residues α274−α291 leading to inactivation of the enzyme. Following protease cleavage in this region, the capacity for bioluminescence activity disbands at a rate identical to the loss of the intact α subunit (*12*). Protease sensitivity is significantly attenuated or abolished following exposure to $FMNH_2$ and O_2, and resistance is maintained much longer after dissolution of the activated FMN intermediate (*13*).

The findings cited above indicate that an intact α subunit unstructured loop is essential to luciferase activity and the catalytic reaction transforms this loop from a resting state to another state or other states more resistant to proteolysis. However, there has no clear evidence as to whether this loop

† Supported by Grant GM25953 from the National Institutes of Health and Grant E-1030 from the Robert A. Welch Foundation.

* Corresponding author: telephone, 713-743-8359; fax, 713-743-8351; e-mail, dtu@uh.edu.

[1] Abbreviations: $FMNH_2$, reduced riboflavin 5′-phosphate; q, quantum; TIM, triose-phosphate isomerase.

10.1021/bi011958p CCC: $22.00
Published on Web 01/17/2002

Scheme 1: Proposed Mechanism for the Bacterial Luciferase Luminescence Reaction

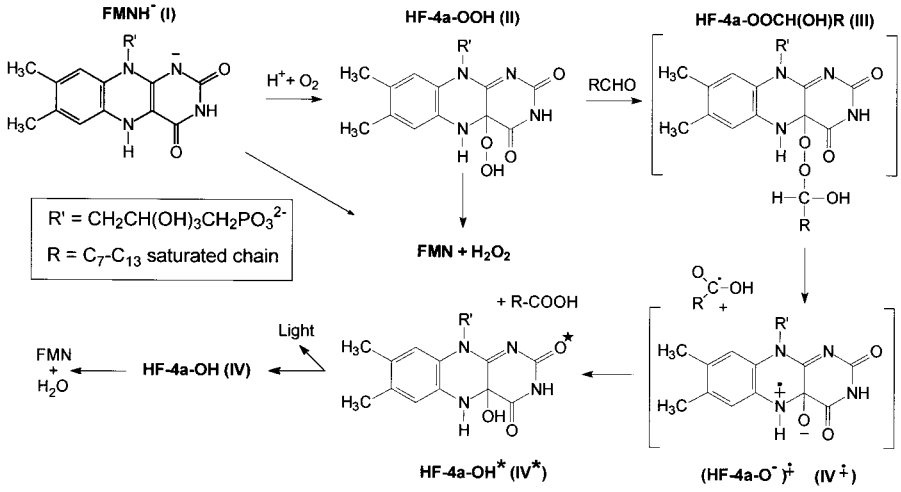

itself is involved in the luciferase catalysis function. In this work, we have performed site-specific mutations of four conserved loop residues identified by sequence alignment using published data (*14*−*19*). The initial mutation of one of these conserved residues reduced the enzyme activity to 1−2% whereas mutations of two other conserved residues resulted in luciferase inactivation by 4−6 orders of magnitude. Each of these two latter residues was mutated to multiple types of residues. The resulting luciferase variants were characterized with respect to steady-state kinetic properties and the yield and stability of the 4a-hydroperoxy-FMN intermediate II by manual mixing and stopped-flow techniques. Results from this work indeed support a critical role of the α subunit unstructured loop in luciferase catalysis. Moreover, two essential residues were shown to have different functional roles. Preliminary results of this work have been reported in the form of an abstract (*20*).

EXPERIMENTAL PROCEDURES

Materials. FMN, decanal, dodecanol, sodium hydrosulfite, and catalase were all from Sigma. Glucose oxidase was from Fluka. Oligonucleotide primers were from MWG Biotech. Wizard SV Plus Miniprep kits and DTT were from Promega. DEAE-cellulose DE52 was from Whatman. All other chromatography resins were from Pharmacia. Stock solutions of decanal were prepared in ethanol. Phosphate (P_i) buffers used were pH 7.0 and were prepared using mole fractions of 0.39 sodium monobase and 0.61 potassium dibase in deionized water. The purity of the enzymes investigated was determined by sodium dodecyl sulfate−polyacrylamide gel electrophoresis (SDS−PAGE).

Luciferase Mutants. Mutagenesis of the wild-type nucleotide sequence of *luxA* was performed using the Stratagene Quickchange mutagenesis kit. The dsDNA template used was the plasmid vector pUC19 harboring the *luxAB* portion of the wild-type *V. harveyi lux* operon. The codon TTT encoding αF261 was modified to TAT, TCT, GCT, and GAT to generate the luciferase mutants αF261Y, αF261S, αF261A, and αF261D, respectively. The codon GGT encoding αG275 was modified to GCT, TTT, ATT, and CCA to generate the mutants αG275A, αG275F, αG275I, and αG275P, accordingly. The codons CGT and GGC encoding residues α278R and α284G, respectively, were modified to GCT and CCC to yield αR278A and αG284P. Each mutant was confirmed following the PCR-based mutagenesis reaction by sequencing purified plasmid DNA from *Escherichia coli* JM109 transformants using the ABI-Prism BigDye sequencing kit.

Enzyme Purification and Activity Assays. The recombinant wild-type and mutant luciferase enzymes were each purified, according to previously described protocols (*21*), from *E. coli* host strain JM109 to >85% homogeneity based on patterns of SDS−PAGE electrophoresis. Bioluminescence activities were measured using a calibrated photometer (*22*) at 23 °C. All reactions were performed in 50 mM P_i buffer unless otherwise stated. Kinetic parameters involving $FMNH_2$ as a substrate for each of the enzyme species were determined using the photoreduction assay described previously (*6*). Decanal kinetic parameters were determined following a modified procedure of the standard Cu(I) assay (*6*, *23*). In each assay, the maximal luminescence intensity was observed immediately following initiation of the reaction by mixing of the enzyme and substrates by manual injection with an airtight syringe. The maximal luminescence intensities (υ) were converted to units of quanta per second (q/s) on the basis of the calibration where one arbitrary unit equals 5.6×10^8 q/s.

4a-Hydroperoxy-FMN Intermediate II Decay. A slight excess of sodium hydrosulfite was added to a solution of 50 mM P_i buffer containing 80 μM FMN and a desired luciferase species. Immediately thereafter, the solution was gently mixed while exposed to the open air. First, the yellow color of the solution was quickly bleached, indicating the initial reduction of FMN, both free and luciferase bound. After a few seconds of mixing, the reducing power of hydrosulfite was exhausted, and the yellow color reappeared, indicating that free $FMNH_2$ reacted with oxygen to regenerate FMN. At the same time, the luciferase-bound $FMNH_2$ also reacted with oxygen to form the 4a-hydroperoxy-FMN intermediate II. The solution was then allowed to stand. The above-described operations were carried out with the sample solutions kept at either 4 or 23 °C. After different incubation times, 100 μL aliquots were withdrawn, and each was injected into 1 mL of 50 mM P_i (kept at 23 °C) containing saturating amounts of decanal substrate to initiate the bioluminescence. The peak luminescence intensity provides a measure of the amount of active intermediate II present

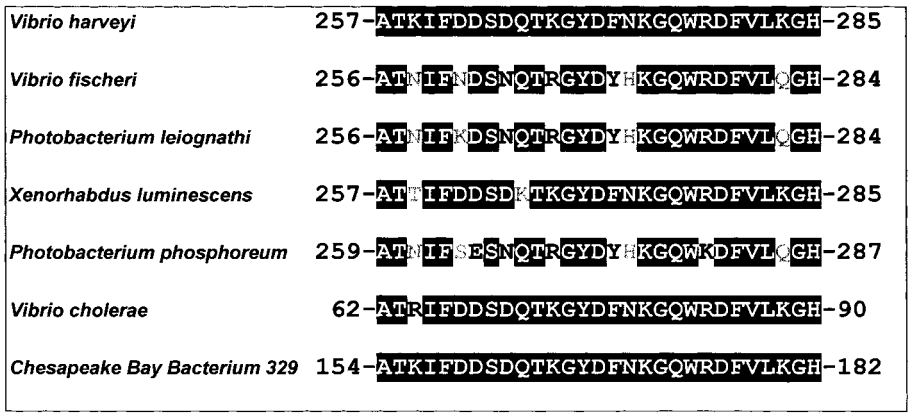

FIGURE 1: Sequence alignment of unstructured loop regions of bacterial luciferase and related proteins. The top five rows of sequence data (one-letter code) correspond to bacterial luciferase enzymes from homologous species, and the bottom two rows are from enzymes identified in nonluminescent bacteria. White letters highlighted in black background are strictly conserved across all species in relation to *V. harveyi*. Residues highlighted against a white background are either conserved in character (black letters) or are not conserved (gray letters).

after a given time of incubation. The decay rate of the intermediate II species was determined by plotting $\log(I/I_0)$ versus time (minutes), where I_0 represents the maximal light emission at time zero and I represents the maximum emission intensities obtained after different times of incubation. An identical set of experiments was conducted with 75 μM (final concentration) dodecanol included in the original luciferase solution to stabilize the intermediate II species following reduction by dithionite (*24*).

Stopped-Flow Spectroscopy. A 50 mM P_i solution containing 50 μM FMN and 10 mM EDTA (solution A) was made anaerobic by repeated evacuation and equilibration with argon in an airtight sealed glass tonometer. FMN was reduced by exposure to long wavelength UV light (λ = 366 nm). Reduction of FMN was confirmed by the disappearance of the FMN absorption spectral characteristics. The $FMNH_2$-containing solution was withdrawn anaerobically into an airtight stopped-flow syringe. A separate air-equilibrated 50 mM P_i solution containing 135 μM desired luciferase species (solution B) was also drawn into a different syringe. Stopped-flow experiments, at 23 °C, were each initiated by mixing 150 μL of solution A and an equal volume of solution B. The absorption spectra of the mixed solution were collected in the range of 280−510 nm using an Olis USA rapid scanning monochromator.

Quantification of Aldehyde Consumption. The method described previously (*21*) was followed with slight modifications for the quantification of aldehyde consumptions in luciferase-catalyzed reactions. A 1 mL buffer solution containing 50 μM $FMNH_2$ [obtained by Cu(I) reduction] was injected into an equal volume of buffer containing 1 μM decanal and 15 μM wild-type luciferase or 25 μM mutant luciferase. After the completion of the bioluminescence reactions, 20 μL aliquots were withdrawn for the determination of remaining amounts of decanal as described previously (*21*).

RESULTS

Mutations of the Unstructured Loop Region. Sequence analysis reveals that the amino acids corresponding to residues 257−285 of the *V. harveyi* luciferase α subunit are highly conserved among all known bacterial luciferase species (Figure 1). Various mutations were performed in this region to examine possible functional roles of the loop and some of its constituent amino acid residues. For the initial study, the conserved residues at position 261, 275, 278, and 284 were each mutated to a single altered residue to obtain luciferase variants αF261D, αG275P, αR278A, and αG284P. When the recombinant plasmids harboring these four mutated luciferases were each expressed in *E. coli* JM109 host cells, all of the mutants except αR278A showed marked decreases in their in vivo luminescence activity. Hence, the αR278A luciferase mutant was not subjected to any further investigation. The αF261D, αG275P, and αG284P mutants plus additional luciferase variants of αF261Y, αF261A, αF261S, αG275F, αG275I, and αG275A generated at a later stage of the study were each purified for further characterizations.

Table 1: Kinetic Parameters[a] of *V. harveyi* Luciferase Mobile Loop Mutants

enzyme	K_{mA} (μM)	K_{mF} (μM)	relative V_{max}	relative V_{max}/K_{mF}
wild type	1.0	0.3	1.0	1.0
αG284P	3.7	0.6	1.8×10^{-2}	0.9×10^{-2}
αG275P	1.8	2.2	4.2×10^{-4}	5.7×10^{-5}
αG275F	2.7	41.1	6.6×10^{-2}	4.8×10^{-4}
αG275I	0.4	58.4	1.5×10^{-1}	7.7×10^{-4}
αG275A	2.2	35.8	2.7×10^{-1}	2.3×10^{-3}
αF261D	4.6	7.5	3.7×10^{-5}	1.5×10^{-6}
αF261S	0.4	36.9	1.3×10^{-3}	1.1×10^{-5}
αF261A	1.7	28.1	1.9×10^{-3}	2.0×10^{-5}
αF261Y	1.6	19.2	3.2×10^{-2}	5.0×10^{-4}

[a] K_{mA} and K_{mF} are Michaelis constants for decanal aldehyde and $FMNH_2$, respectively.

Kinetic Parameters of Three Loop Mutants. Mutants αG284P, αG275P, and αF261D were first analyzed to determine their V_{max} and Michaelis constants (Table 1). In comparison with the wild-type luciferase, the Michaelis constants for the $FMNH_2$ (K_{mF}) and decanal (K_{mA}) substrates for all three mutants were significantly but not drastically increased. The V_{max} of αG284P was reduced to 1.8% of the native enzyme level. Remarkably, 4 and 5 orders of magnitude of reductions in V_{max} were observed with αG275P and αF261D, respectively (Table 1). Comparisons of V_{max}/K_{mF} (Table 1) and V_{max}/K_{mA} (not shown) reveal the same general pattern. Such findings clearly indicate that the structural integrities of αG284 and, especially, αG275 and αF261 are highly critical to *V. harveyi* luciferase activity.

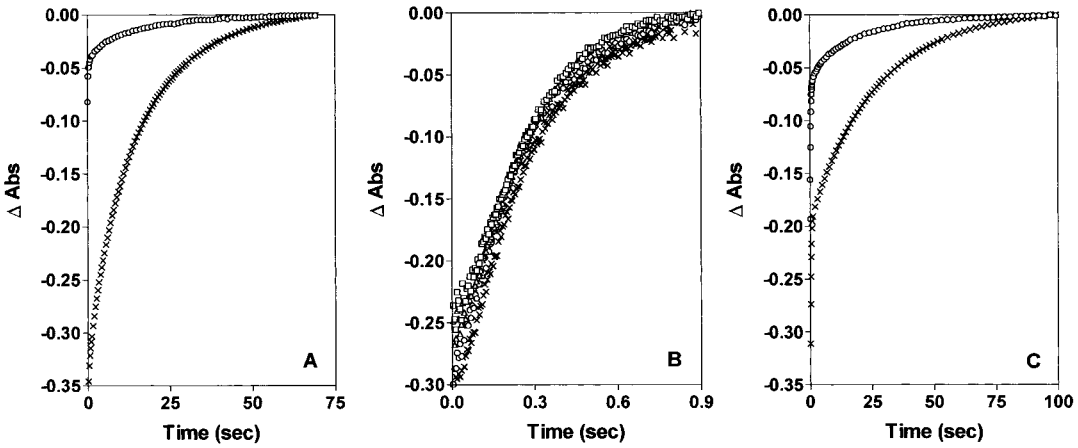

FIGURE 2: Comparison of time courses of $FMNH_2$ oxidation by either autoxidation or enzyme-catalyzed oxidation using luciferase mutants αF261D or αG275P. In all panels, a solution of 50 mM phosphate buffer (pH 7.0) containing 50 μM FMN and 10 mM EDTA (with or without the desired luciferase species) was made anaerobic by successive rounds of argon evacuation. Using an Olis USA stopped-flow spectrophotometer, the respective solutions were mixed with an equal volume of air-equilibrated 50 mM phosphate buffer. Monitoring ΔA_{382} and ΔA_{445} as a function of time assessed $FMNH_2$ oxidation, and the final absorbance readings (A_{final}) of the fully oxidized solutions were used as a reference. Changes in respective absorbance are represented as $A - A_{final}$. (A) $FMNH_2$ oxidation by αG275P monitoring ΔA_{382} (○) and ΔA_{445} (×). (B) Comparison of rapid $FMNH_2$ autoxidation [ΔA_{382} (□) and ΔA_{445} (△)] versus oxidation by αF261D [ΔA_{382} (○) and ΔA_{445} (×)]. ΔA values in panel B were multiplied by 2.0 (○), 1.59 (□), and 1.716 (×) for direct graphic comparison. (C) Long time-course oxidation of $FMNH_2$ by αF261D. Symbols used are identical to those described in panel A.

Table 2: Dark Decay Rates of Intermediate II Derived from Native Enzyme and Luciferase Variants

	decay rate (min^{-1})			
enzyme	23 °C	4 °C	23 °C + dodecanol	4 °C + dodecanol
wild type	3.7	0.08	0.11	0.03
αG275P	4.0	0.12	0.16	0.12
αF261D	7.7	0.14	0.63	0.26

The latter two luciferase variants were subjected to further characterizations.

Stability of 4a-Hydroperoxy-FMN Intermediates. As shown in Scheme 1, intermediate II can either react with the appropriate aldehyde substrate to promote the light emitting reaction or decay to yield FMN and H_2O_2 by a nonradiative mechanism. The stability of intermediate II of the native luciferase can be enhanced at lower temperatures or by forming a complex with a long-chain alcohol, which is a competitive inhibitor to the aldehyde substrate (*24*). The intermediate II decay rates at 23 and 4 °C in the absence and presence of 75 μM dodecanol for the native luciferase were determined again in this work as controls for comparisons with those of αG275P and αF261D (Table 2). Although in some cases the differences were marginal, generally the stabilities of the intermediate II species decreased from the wild-type luciferase to αG275P and then to αF261D under all conditions examined. It should be noted that >10-fold stabilizations of intermediate II by complex formation with dodecanol were observed for intermediate II of wild type, αG275P, and αF261D at 23 °C. At 4 °C, dodecanol provided a small degree of stabilization of the native luciferase intermediate II but no stabilization of the αG275P intermediate II. For αF261D at 4 °C, dodecanol even destabilized intermediate II by about 2-fold.

Stopped-Flow Measurements of $FMNH_2$ Oxidation. FMN and luciferase intermediate II share an absorption isosbestic point at 382 nm, and the level of absorption at that wavelength is approximately twice that of $FMNH_2$ (*21*). Moreover, FMN displays a high level of absorption whereas $FMNH_2$ and intermediate II both absorb very weakly at 445 nm. Therefore, the conversion of $FMNH_2$ to intermediate II can be characterized by an initial sizable increase in absorbance at 382 nm with little increase in absorption at 445 nm. Following its formation, the decay of intermediate II is characterized by an increase in absorbance at 445 nm with no further change in the level of absorption at 382 nm. These spectral characteristics were exemplified when wild-type luciferase was utilized for the catalytic oxidation of $FMNH_2$ in our previous study (*25*) and in this work (data not shown). In contrast, autoxidation of $FMNH_2$ does not involve any detectable formation of the intermediate II species (*26*). Accordingly, the conversion of the reduced to the fully oxidized flavin by autoxidation is typified by parallel increases in the levels of absorption at 382 and 445 nm (Figure 2B). Therefore, comparisons of the time courses of ΔA_{445} and ΔA_{382} provide a convenient means to investigate the involvement or lack of intermediate II in $FMNH_2$ oxidation catalyzed by luciferase variants. Such an approach was employed in a series of stopped-flow experiments to determine the effects of mutations on the abilities of αF261D and αG275P in forming intermediate II. The kinetics of reduced flavin autoxidation (*27*) and luciferase-catalyzed oxidation (*28*) are both quite complex. The present study aimed at the detection of intermediate II; detailed kinetic analyses of reaction steps and rate constants were not intended.

The intermediacy of II was first examined in a reaction initiated by mixing an anaerobic solution containing 50 μM $FMNH_2$ with an equal volume of air-saturated solution containing 135 μM αG275P. As shown in Figure 2A, a rapid and large rise of A_{382} was observed immediately after the onset of the reaction while very little increase of A_{445} was detected. This phase was followed by a large, slower, and apparently first-order rise of A_{445} accompanied by only small increases in A_{382}. These characteristics are quite similar to those observed with the native luciferase-catalyzed oxidation

of $FMNH_2$ (*25*), indicating that intermediate II was indeed formed during the oxidation of $FMNH_2$ in the presence of αG275P. On the basis of the patterns of ΔA_{382} and ΔA_{445} time courses, the initial rapid phase corresponds to the formation of intermediate II from $FMNH_2$ whereas the second and slow phase corresponds to primarily the decay of intermediate II to FMN. In accord with such a conclusion is that the apparent first-order rate constant of 5.0 min^{-1} determined from the ΔA_{445} time course in Figure 2A corresponds reasonably well with the 4.0 min^{-1} decay rate of intermediate II determined by activity assay (Table 2). In our past experience, the yields of intermediate II by the wild-type luciferase under similar conditions were ≥80% (*25*). On the basis of the maximal ΔA_{445} and the theoretical initial level of 25 μM $FMNH_2$ immediately after mixing, the results shown in Figure 2A gave rise to an estimated intermediate II yield of about 62%.

Similar experiments using αF261D showed a more complex pattern of $FMNH_2$ oxidation. The kinetic pattern of the first 0.9 s after mixing was analyzed in more detail. As mentioned above, the time courses of ΔA_{445} and ΔA_{382} paralleled each other in the autoxidation of free $FMNH_2$ with the same apparent first-order rate constant of 3.0 s^{-1} (Figure 2B). The initial time courses of ΔA_{445} and ΔA_{382} also paralleled each other in the oxidation of $FMNH_2$ in the presence of αF261D, with respective apparent first-order rate constants of 3.0 and 3.7 s^{-1}, similar to that of autoxidation (Figure 2B). These results indicate that the $FMNH_2$ oxidation in the presence of αF261D involved autoxidation. The $FMNH_2$ oxidation time courses were also examined on a longer time scale similar to that in Figure 2A. Results shown in Figure 2C revealed not only a large and rapid initial rise in A_{382} but also a significant rapid rise in A_{445} within the first second, attributable to the autoxidation of $FMNH_2$ described under Figure 2B. Subsequently, a large and slower rise phase was detected with the ΔA_{445} time course whereas a much smaller rise of ΔA_{382} was observed during the same phase. The time course of ΔA_{445} can be fitted as a double exponential with a minor and fast phase of $k = 2.7$ s^{-1} attributed to residual $FMNH_2$ autoxidation and a slow major phase of $k = 2.3$ min^{-1} attributed to intermediate II formation. On the basis of actual absorbance changes (rather than normalized values shown in Figure 2), 36% of the total $FMNH_2$ was estimated to undergo intermediate II formation with the rest autoxidized. A possibility that cannot be eliminated is that the autoxidation mentioned above was actually catalyzed by αF261D in a process that did not involve intermediate II and fortuitously had a rate constant similar to that of autoxidation. In any case, it is clear that αF261D is capable of generating intermediate II but, under our experimental conditions, with a lower yield than those of the wild-type luciferase and αG275P.

Aldehyde Consumption. The formation of the exited emitter in the luciferase bioluminescence reaction is coupled to the oxidation of aldehyde to acid. Using a sample containing limiting decanal and excess amounts of both $FMNH_2$ and wild-type luciferase as a positive control, 16 ± 3% of the initial amount of decanal was detected unconsumed after cessation of the luciferase-catalyzed luminescence reaction. When αG275P and αF261D were used in place of the native luciferase, 82 ± 9% and 90 ± 16%, respectively, of decanal were recovered after the bioluminescence reaction.

Kinetic Parameters of Additional αG275 and αF261 Mutants. Additional mutations of αG275 and αF261 were carried out for a more thorough investigation of the functional roles of these two residues. In comparison with the wild-type luciferase, the four αG275-mutated and the four αF261-mutated luciferase variants showed relatively little changes in their K_{mA} but significantly wider ranges of increases in their K_{mF} (Table 1). Hence, values of V_{max} and V_{max}/K_{mF}, but not V_{max}/K_{mA}, for all mutants are also included in Table 1 for comparison. For V_{max} and V_{max}/K_{mF} of the αG275-mutated enzymes, 4−5 orders of magnitude of reductions were detected with αG275P. Gradual but partial recoveries of the lost activities were detected when the αG275 mutation was changed from proline to the neutral residues phenylalanine, isoleucine, and alanine with progressive decreases in the size of their respective side chain. For the αF261-mutated enzymes, the mutation of phenylalanine to the anionic aspartyl residue resulted in the largest degrees of reduction in V_{max} and V_{max}/K_{mF} to levels about 5 orders of magnitude lower than those of the wild-type luciferase. Such dramatic levels of reduction in V_{max} and V_{max}/K_{mF} were progressively but partially reverted when αF261 was mutated to the hydrophilic serine, the aliphatic alanine, and the aromatic tyrosine residue. In terms of V_{max}, the αF261Y variant was only 30-fold lower than that of the wild-type luciferase.

DISCUSSION

Bacterial luciferase belongs to a family of enzymes described as αβ-barrel enzymes (or TIM barrel enzymes) first observed in the structure of triose-phosphate isomerase (TIM) (*29*). Within this family of enzymes, bacterial luciferase is in a class with other αβ-barrel enzymes that bind FMN, which includes old yellow enzyme (*30*), glycolate oxidase (*31*), flavocytochrome b_2 (*32*), and trimethylamine dehydrogenase (*33*). Bacterial luciferase differs from the aforementioned enzymes in that it does not contain FMN as a tightly bound cofactor but binds $FMNH_2$ as a substrate. The structural design of the αβ-barrel is such that eight repeating sections of the β-sheet−loop−α-helix motif, each connected by an intervening loop, fold to form a barrel-shaped core of parallel β-sheets confined by a solvent-exposed cage of α-helices (*34*).

The *V. harveyi* luciferase α subunit contains a long stretch of loop connecting its α7a-helix to the β7a-sheet (*8*). Within this long loop, a 29-residue segment from α258 to α286 is missing from the primary sequence of β, and residues α272−288 and α262−290 are respectively not resolved in the 2.4 and 1.5 Å crystal structures of the native enzyme (*8, 9*). This feature constitutes a major structural distinction between the α and β subunits in all bacterial luciferases. Similar loops are frequently observed in this or analogous positions in the family of TIM barrels and have been examined in great detail (*35*−*38*). Previously, Baldwin et al. have hypothesized that the unstructured loop acts as a shield for catalytic intermediates (*2*). The work reported here was initiated to experimentally examine the possible involvement of the unstructured loop in the catalytic function of *V. harveyi* luciferase and to determine the identity and function of specific amino acid residue(s) within this loop that is/are essential to luciferase catalysis.

Three luciferase variants (namely, αG284P, αG275P, and αF261D), each with mutation of a different conserved residue

within the α subunit unstructured loop, were initially purified for characterizations. All three luciferase variants showed markedly reduced V_{max} and V_{max}/K_{mF}, ranging from a few percent to 10^{-6} of those of the native luciferase (Table 1). These findings clearly indicate an essential role of the unstructured loop in the expression of luciferase catalytic activity and suggest that these three conserved residues may have specific functional roles in catalysis. In view of the highly pronounced activity reductions shown by αG275P and αF261D, additional mutations at these positions were carried out to more thoroughly probe the functionalities of αG275 and αF261.

On the basis of Scheme 1 and as rationalized before (*25*), the overall quantum yield (Φ_o) of the luciferase-catalyzed reaction can be related to a set of yields:

$$\Phi_o = Y_{II}Y_{III}Y_{IV^+\bullet}Y_{IV^*}\Phi_{IV^*} \quad (1)$$

where each *Y* refers to the yield of a particular intermediate (indicated by the subscript) on the basis of its immediate precursor intermediate and Φ_{IV^*} is the intrinsic emission quantum yield of the excited intermediate IV*. This relationship will be followed for the analysis of the functional consequences of mutations of αG275 and αF261.

On the basis of stopped-flow results (Figure 2), both αG275P and αF261D were capable of generating intermediate II with yields estimated to be 62% and 36%, respectively. While these yields are significantly lower than that of the native luciferase, the decreases in Y_{II} are substantially below the 4−6 orders of activity reductions shown by αG275P and αF261D. For the next step of the reaction, intermediate II either reacts with aldehyde to form intermediate III or undergoes a competing dark decay to produce FMN and H_2O_2. Enhanced dark decay rates of the intermediate II species derived from αG275P and αF261D were detected in comparison with the native enzyme intermediate II at two different temperatures and in the absence or presence of dodecanol as a stabilization agent (Table 2). These enhanced dark decays could reduce the yields of intermediate III (i.e., Y_{III}) but, again, at levels much lower than the overall reductions of Φ. The formation of intermediate $IV^{+\bullet}$ and, in turn, IV* is coupled to the oxidation of the aldehyde substrate. While quantitative measurements of $Y_{IV^+\bullet}$ or Y_{IV^*} were not achieved, 82−90% of the initial aldehyde substrate was found unconsumed by αG275P and αF261D, respectively, in comparison with 16% by the native luciferase. Taking into consideration the error margins (9−16% for the two mutants), these findings indicate that the abilities of these two mutants to oxidize aldehyde are substantially compromised. Again, our results do not allow a direct quantification of Φ_{IV^*} for the two mutants. The Φ_{IV^*} of the excited emitter IV* bound to the native luciferase has been estimated to be 0.18 (*39*), which is 4 orders of magnitude higher than the fluorescence quantum yield of a free 4a-hydroxyflavin model (*40*). Clearly, the nature of IV* binding to luciferase is highly critical to the expression of Φ_{IV^*}. Conceivably, mutations of either of the conserved and essential αG275 and αF261 could change the microenvironment of the emitter binding site, thus resulting in markedly reduced Φ_{IV^*}. In view of the above discussions, it is most likely that the drastically reduced bioluminescence activities of αG275P and αF261D are compound consequences of the mutational effects on Y_{II}, Y_{III}, $Y_{IV^+\bullet}$, Y_{IV^*}, and Φ_{IV^*}, with the latter three factors potentially contributing much more than the former two factors to the markedly reduced Φ.

The αG275 residue is at the center of the unstructured loop region of the *V. harveyi* luciferase α subunit. A similar loop structure has been observed in TIM, and the motion of loop transition has been characterized (*37*). It is not known for certainty whether such type of loop movement observed in TIM and other enzymes (*41*, *42*) applies the luciferase unstructured loop. However, the high sensitivity of this loop to proteolysis can be greatly reduced by binding of phosphate (*43*, *44*) and by reacting luciferase with the $FMNH_2$ and O_2 substrates with the protecting effect lasting beyond the removal of the bound flavin (*13*). On the basis of these data, Baldwin et al. (*2*) have suggested multiple conformations of the unstructured loop. Our results not only support such a conjecture but also indicate an essential functionality of the structural flexibility of the loop region. When the highly flexible αG275 is mutated to the rigid proline, the luciferase activity was reduced remarkably by 4−5 orders of magnitude in terms of V_{max} and V_{max}/K_{mF}. The lost activities were progressively but partially recovered when αG275 was mutated to phenylalanine, isoleucine, and alanine with increasing degrees of freedom for torsional flexibility. The exact functional role of the proposed loop mobility in luciferase bioluminescence catalytic activity cannot be deduced from the present results. However, we entertain the possibility that the loop may serve as a gating mechanism. At some point after the binding of the substrates, the loop could conceivably change from an initial open conformation to a closed conformation to reduce or prevent accessibility of the active site to the aqueous medium. Model studies have revealed that the dark decay of 4a-hydroperoxyflavin compounds can be effectively retarded in a more hydrophobic environment (*45*). The binding of hydrophobic long-chain alcohols to the native luciferase markedly stabilize intermediate II (*24*). Hence, a closed conformation of the loop is likely to enhance the formation of intermediate III from intermediate II and aldehyde by reducing the dark decay of intermediate II and may possibly even lead to better $Y_{IV^+\bullet}$ and/or Y_{IV^*}. Moreover, considering the remarkable reduction of the 0.18 Φ_{IV^*} of the luciferase-bound emitter (*39*) to a level of 10^{-5} for the fluorescence quantum yield of free 4a-hydroxyflavin (*40*), a minimization of solvent accessibility of the active site achievable by the closed conformation of the loop may be critical in ensuring a high quantum yield of the luciferase emitter. The essentiality of the flexible αG275 and, to a lesser degree, αG284 in the loop is certainly consistent with such an interpretation.

A comparison of the properties of αF261D, αF261S, αF261A, and αF261Y indicates that the essentiality of αF261 is associated with the high hydrophobicity and the bulkiness of the phenyl side chain of this residue. A correlation was observed between the decreasing size and hydrophobicity of the side chain at α261 and the diminution of observed V_{max} and V_{max}/K_{mF}. Compared to the native enzyme, the mutant αF261Y was only slightly affected by the addition of the *p*-hydroxyl group on the phenyl group of the side chain. Further decreases in V_{max} and V_{max}/K_{mF} were observed in the order of αF261A, αF261S, and αF261D when the phenyl group was replaced by respectively a hydrophobic

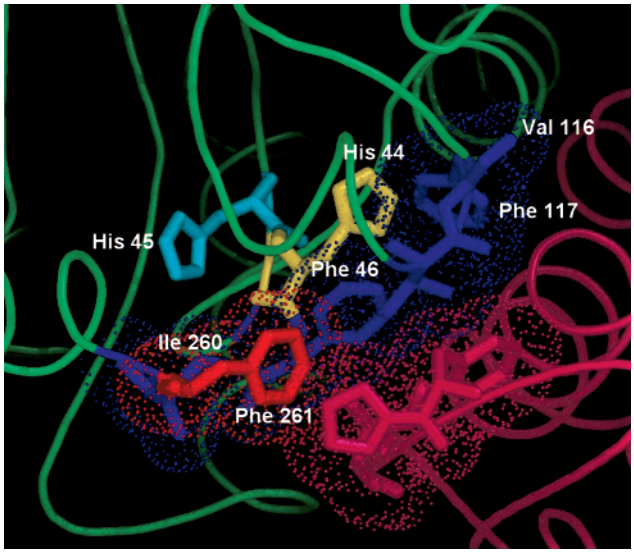

FIGURE 3: Residue αF261 as a component of a hydrophobic barrier that shields the proposed catalytic site. Wire-frame representations of luciferase α and β subunit secondary structures are shown in green and magenta, respectively. αF261 is colored in red and is a component of a hydrophobic layer comprised of α subunit residues F46, I260, V116, and F117 (each shown in blue). This hydrophobic layer in the α subunit may shield the proposed luciferase active site, which includes the essential αHis44 (yellow) and αHis45 (cyan), from solvent accessibility. Additional nearby hydrophobic residues (colored in magenta) in the β subunit may also contribute to such a shielding effect. van der Waals surfaces are represented by dots for each of the hydrophobic side chains depicted.

but smaller methyl, a hydrophilic hydroxymethyl, and an anionic alkyl carboxylate group.

The high-resolution crystal structure of the native enzyme (*9*) reveals (Figure 3) that the αF261 side chain is approximately 4 Å from the phenyl ring of αF46 and protrudes toward the interior of the enzyme near the essential residues αH44 and αH45. Both residues are part of the hypothesized luciferase active site (*8*), with αH45 being essential to the formation of intermediate II (*7*, *25*) and αH44 functioning as a catalytic base required for step(s) after intermediate II formation (*7*, *25*). In addition, αF261 packs well with residues αI260, αV116, and αF117 to form a tight, hydrophobic barrier that could serve as a shield protecting the hypothesized active site against exposure to the solvent. As mentioned above, a hydrophobic environment of the luciferase active site during catalysis may contribute to reduced dark decay of intermediate II, enhanced yield of intermediate III, and a likely significant enhancement of the emitter Φ_{IV^*}. Hence, αF261 may function in any one or any combination of these processes in luciferase catalysis. The mutation of αF261 to an aspartyl residue indeed showed, in addition to a decreased yield of intermediate II, enhanced nonproductive dark decay of intermediate II at two temperatures with or without the presence of dodecanol (Table 2) and decreased oxidation consumption of aldehyde substrate.

In this paper we report that components of the unstructured loop, and the loop as a whole, are intimately involved in the luciferase bioluminescence catalytic activity. Analysis of mutants of αF263 and αG275 indicates that these two conserved residues are involved in different aspects of the catalytic cycle.

ACKNOWLEDGMENT

We thank Dr. John Olson and Dr. Tony Matthews at Rice University for the use of equipment and consultation in obtaining the stopped-flow data reported in this work.

REFERENCES

1. Tu, S. C., and Mager, H. I. (1995) *Photochem. Photobiol. 62*, 615−624.
2. Baldwin, T. O., Christopher, J. A., Raushel, F. M., Sinclair, J. F., Ziegler, M. M., Fisher, A. J., and Rayment, I. (1995) *Curr. Opin. Struct. Biol. 5*, 798−809.
3. Baldwin, T. O., Ziegler, M. M., and Powers, D. A. (1979) *Proc. Natl. Acad. Sci. U.S.A. 76*, 4887−4889.
4. Meighen, E. A., and Hastings, J. W. (1971) *J. Biol. Chem. 246*, 7666−7674.
5. Becvar, J. E., and Hastings, J. W. (1975) *Proc. Natl. Acad. Sci. U.S.A. 72*, 3374−3376.
6. Lei, B., Cho, K. W., and Tu, S. C. (1994) *J. Biol. Chem. 269*, 5612−5618.
7. Huang, S., and Tu, S. C. (1997) *Biochemistry 36*, 14609−14615.
8. Fisher, A. J., Raushel, F. M., Baldwin, T. O., and Rayment, I. (1995) *Biochemistry 34*, 6581−6586.
9. Fisher, A. J., Thompson, T. B., Thoden, J. B., Baldwin, T. O., and Rayment, I. (1996) *J. Biol. Chem. 271*, 21956−21968.
10. Johnston, T. C., Thompson, R. B., and Baldwin, T. O. (1986) *J. Biol. Chem. 261*, 4805−4811.
11. Cohn, D. H., Mileham, A. J., Simon, M. I., Nealson, K. H., Rausch, S. K., Bonam, D., and Baldwin, T. O. (1985) *J. Biol. Chem. 260*, 6139−6146.
12. Baldwin, T. O., Hastings, J. W., and Riley, P. L. (1978) *J. Biol. Chem. 253*, 5551−5554.
13. AbouKhair, N. K., Ziegler, M. M., and Baldwin, T. O. (1985) *Biochemistry 24*, 3942−3947.
14. Foran, D. R., and Brown, W. M. (1988) *Nucleic Acids Res. 16*, 777.
15. Lee, C. Y., Szittner, R. B., and Meighen, E. A. (1991) *Eur. J. Biochem. 201*, 161−167.
16. Ferri, S. R., Soly, R. R., Szittner, R. B., and Meighen, E. A. (1991) *Biochem. Biophys. Res. Commun. 176*, 541−548.
17. Xi, L., Cho, K. W., and Tu, S. C. (1991) *J. Bacteriol. 173*, 1399−1405.
18. Palmer, L. M., and Colwell, R. R. (1991) *Appl. Environ. Microbiol. 57*, 1286−1293.
19. Ramaiah, N., Chun, J., Ravel, J., Straube, W. L., Hill, R. T., and Colwell, R. R. (2000) *FEMS Microbiol. Ecol. 33*, 27−34.
20. Low, J. C., and Tu, S.-C. (2000) 13th International Congress on Photobiology, Abstract 360.
21. Xin, X., Xi, L., and Tu, S. C. (1991) *Biochemistry 30*, 11255−11262.
22. Hastings, J. W., and Weber, J. (1963) *J. Opt. Soc. Am. 53*, 1410−1415.
23. Lei, B. F., and Becvar, J. E. (1991) *Photochem. Photobiol. 54*, 473−476.
24. Tu, S. C. (1979) *Biochemistry 18*, 5940−5945.
25. Li, H., Ortego, B. C., Maillard, K. I., Willson, R. C., and Tu, S. C. (1999) *Biochemistry 38*, 4409−4415.
26. Hastings, J. W., and Gibson, Q. H. (1967) *J. Biol. Chem. 242*, 720−726.
27. Gibson, Q. H., and Hastings, J. W. (1962) *Biochem. J. 83*, 368−377.
28. Abu-Soud, H. M., Clark, A. C., Francisco, W. A., Baldwin, T. O., and Raushel, F. M. (1993) *J. Biol. Chem. 268*, 7699−7706.
29. Banner, D. W., Bloomer, A. C., Petsko, G. A., Phillips, D. C., Pogson, C. I., Wilson, I. A., Corran, P. H., Furth, A. J., Milman, J. D., Offord, R. E., Priddle, J. D., and Waley, S. G. (1975) *Nature 255*, 609−614.
30. Fox, K. M., and Karplus, P. A. (1994) *Structure 2*, 1089−1105.
31. Lindqvist, Y. (1989) *J. Mol. Biol. 209*, 151−166.

32. Xia, Z. X., and Mathews, F. S. (1990) *J. Mol. Biol. 212*, 837−863.
33. Lim, L. W., Shamala, N., Mathews, F. S., Steenkamp, D. J., Hamlin, R., and Xuong, N. H. (1986) *J. Biol. Chem. 261*, 15140−15146.
34. Farber, G. K., and Petsko, G. A. (1990) *Trends Biochem. Sci. 15*, 228−234.
35. Brzovic, P. S., Hyde, C. C., Miles, E. W., and Dunn, M. F. (1993) *Biochemistry 32*, 10404−10413.
36. Lundqvist, T., and Schneider, G. (1991) *J. Biol. Chem. 266*, 12604−12611.
37. Joseph, D., Petsko, G. A., and Karplus, M. (1990) *Science 249*, 1425−1428.
38. McMillan, F. M., Cahoon, M., White, A., Hedstrom, L., Petsko, G. A., and Ringe, D. (2000) *Biochemistry 39*, 4533−4542.
39. Tu, S. C. (1982) *J. Biol. Chem. 257*, 3719−3725.
40. Kaaret, T. W., and Bruice, T. C. (1990) *Photochem. Photobiol. 51*, 629−633.
41. Janin, J., and Wodak, S. J. (1983) *Prog. Biophys. Mol. Biol. 42*, 21−78.
42. McCammon, J. A., Gelin, B. R., Karplus, M., and Wolynes, P. G. (1976) *Nature 262*, 325−326.
43. Holzman, T. F., and Baldwin, T. O. (1980) *Biochem. Biophys. Res. Commun. 94*, 1199−1206.
44. Holzman, T. F., and Baldwin, T. O. (1980) *Proc. Natl. Acad. Sci. U.S.A. 77*, 6363−6367.
45. Kemal, C., and Bruice, T. C. (1976) *Proc. Natl. Acad. Sci. U.S.A. 73*, 995−999.

BI011958P